PROGRESS REPORT,

~~Covering Period from~~

15 October 1966 to 15 April 1967

RADIATION DAMAGE TO SEMICONDUCTORS BY HIGH ENERGY ELECTRONS

John C. Corelli

Sponsored by the National Aeronautics and Space Administration

Under Grant NsG-290

Department of Nuclear Engineering and Science.

Rensselaer Polytechnic Institute

Troy, New York

CONTENTS

		Page
I.	Introduction.....	1
II.	Brief Discussion of Status of Experimental Programs.....	2
	1. Low Temperature Stress Dewar for Optical Measurements - A. H. Kalma.....	2
	2. Photoconductivity of Silicon - A. H. Kalma....	2
	3. Impurity Associated Radiation - Induced Defects in Silicon - R. Edelstein.....	7
	4. Saturation of the Fermi Level in Germanium Irradiated to High Doses of $\approx$50 MeV Electrons ($\sim$5-10 x 10^{18} e/cm^2) - W. Bohlke...	10
III.	Research Plans for the Next Six Month Period.....	19
	References.....	20
	Figures.....	21

I. Introduction

In this progress report we shall present results of our program obtained during the six month period 15 October 1966 to 15 April 1967. We shall only give brief status reports of the work and a brief mention of some plans for future experiments. The following personnel were actively engaged in the research program:

Faculty:

Dr. John C. Corelli (half time October-November, 1966; 3/4 time December 1966 - April 1967)

Graduate Students

Mr. Arne H. Kalma (NASA Fellow)

Mr. William Bohlke

Mr. Robert Edelstein (AEC Fellow)

Research Technician

Mr. James Westhead

Some of our results on the optical properties of irradiated silicon have appeared in a recent paper entitled: "1.8-, 3.3-, and 3.9-μ Bands in Irradiated Silicon: Correlations With the Divacancy", L. J. Cheng, J. C. Corelli, J. W. Corbett and G. D. Watkins; Phys. Rev. 152, 761 (1966). Reprint copies of the above paper are attached at the end of the report.

II. Brief Discussion of Status of Experimental Programs

1. Low Temperature Stress Dewar for Optical Measurements - A. H. Kalma

During the past six month period the dewar and stressing apparatus were received from the manufacturer.* The dewar is capable of operation in the liquid helium temperature range and will be used in optical studies at wavelengths below 6μ the cutoff of the cold sapphire window of the dewar. A substantial effort during the end of the present report period was to build the external stress apparatus that is used in conjunction with the dewar. We anticipate that the stress dewar will be ready for use during the coming summer 1967, a delay caused by lack of available experienced manpower. The stressing apparatus was designed to be inserted inside the dewar as a separate component. The maximum force which can be exerted on a sample within design limits is ~400 lbs.

2. Photoconductivity of Silicon - A. H. Kalma

A. Introduction

Photoconductivity studies of electron-irradiated n-type silicon are being performed to look at the defect energy levels that are introduced. These studies are being carried out to attempt to identify the defects that are giving rise to the various energy levels. The methods being used are dopant studies (both type and concentration), annealing studies, and stress-

---

*Andonian Associates, Inc., Waltham, Massachusetts.

induced dichroism studies. Other methods, such as bleaching, with light, are contemplated for the future.

B. Experimental Description

Thus far, most of the samples used have been 100 Ωcm, although a few 10 Ω cm ones have been studied. All samples were prepared from low oxygen containing ($\lesssim 10^{16}$ oxygen/cm^3) zone-refined material. The samples are rectangular bars whose dimensions are about 15 mm x 3 mm x 2 mm. The contacts are put on by heating and pressing arsenic-doped gold into the ends of one of the faces. The ends of the sample are polished flat and parallel for stressing. The irradiations were carried out at room temperature with 45-50 MeV electrons. The 100 Ω cm samples received total integrated fluxes of between 1.0×10^{14} and 1.5×10^{14} electrons/cm^2 and the 10Ωcm ones received 10^{15} electrons/cm^2. The photoconductivity spectra are measured at 80^{o}K. The total integrated fluxes used in these experiments were high enough to drive the resistance of the samples from a few hundred ohms before irradiation to 10^6-10^{11} ohms after irradiation. In some of the first studies to be reported here the input impedance of the equipment was only 2×10^7 ohms causing large signal loss.

We are currently using a Keighley Model 610A electrometer having an input impedance of 10^{14} ohms as a unity gain pre-amplifier to allow for these high sample resistances.

We have been using a Perkin-Elmer model 107 amplifier and a home made high sensitivity, low noise preamplifier to pick up the

signal. We now have on order a Princeton Applied Research Model HR-8 lock in amplifier and associated high impedance preamplifier. This will allow us to detect signals in the nanovolt range according to specifications instead of our current tenths of a microvolt range.

In attempting to perform polarized light studies of stressed samples on our Spex Model 1500 grating monochromator, we discovered that the gratings polarized the light very strongly in certain wavelength regions. This may be due to the light striking the gratings at close to the Brewster angle at certain grating settings. Further study is necessary to see if this is the reason and to determine if there are gratings that will cover the range we are interested in without polarizing the light. Because of this light polarizing problem, we are currently using a Perkin Elmer Model 98 prism monochromator. This instrument was also found to polarize the light but the ratio of $E_{\perp}/E_{\parallel}$ does not exhibit a strong wavelength dependence as was found in our grating monochromator in the 2.5 to 4.5 μ wavelength range.

As this instrument is sitting in air, atmospheric absorptions give unwanted absorptions in certain wavelength ranges and it may be that we can eliminate air absorptions using the evacuable Spex instrument. More study of this problem is needed to determine whether air absorption can be cut down sufficiently in the prism instrument to allow its use. Due to the inherently poorer energy resolution, of a prism instrument any absorption cuts out a higher wavelength region than would occur for a

grating instrument and it appears now that the Spex grating monochromator may be better, especially if better gratings are available.

The annealing work performed thus far has been isochronal for 15 minute time intervals and in all cases the sample was heated in air. In the stress experiments thus far completed we applied the stress on samples kept in an oil bath and heated to $\approx 160^{\circ}C$ for 15 minutes.

C. Results and Discussion

Figure 1 shows a 100Ωcm, As doped sample irradiated with 48 MeV electrons to a total integrated flux of 10^{14} e/cm^2. The temperature labelings are the isochronal annealing temperatures. The $125^{\circ}C$ spectrum values are probably a bit low as the resistance of the sample was only estimated to be greater than 10^8 ohms from an ohmmeter for normalization purposes. There was some pump oil getting on this sample during pump down and absorbing between 2.8 μ and 3.2 μ. Therefore, the spectra in this region are only approximate.

Figure 2 shows the annealing results for this sample. The E_c -.60 eV level appears to be in slightly different places before and after its near disappearance at $160^{\circ}C$. It has been drawn as one level here but may in fact be two separate ones. It is not known whether the level giving rise to photoconductivity at 1.45 μ is located at E_v + .83 eV or E_c - .83 eV. This is indicated in the level diagram in the figure. The photoconductivity peak centered at 4.45 μ is believed to be associated with a

defect, further work is in progress. The 4.45 μ peak has been found on a few other samples. The region where the photoconductivity signal would have to be diminished by absorption is quite broad (over 1 μ) and no material or combination of materials in our apparatus (such as vacuum grease, pump oil, atmosphere, etc.) will absorb for the entire region. Also, the Fermi level was probably deeper than 0.26 eV below the conduction band when the peak was observed and did not rise that high until after some annealing had occurred at 160°C, after which no peak was observed. This last reason comes from the measured DC resistance of the sample at 80°K and a rough estimate or the Fermi level position.

Figure 3 shows the spectra of 100 Ωcm phosphorus doped sample after various anneals. This sample was irradiated with 48 MeV electrons to a total integrated flux of 1.4×10^{14} electrons/cm^2. Figure 4 summarizes the annealing results of this sample. This sample has not been completely annealed to date. As on the previous sample, the positioning of the level giving rise to photoconductivity at 1.45 μ is in question, as the defect energy level diagram shows.

Figure 5 shows the spectra of a 100 Ωcm, antimony doped sample that has been stressed with 1400 kg/cm^2 along the [011] direction. The signal from the sample was low and fairly noisy and therefore the accuracy of the points isn't as good as would be wanted. These spectra were also taken on our Spex grating instrument causing further uncertainty. Even so, the spectra taken with unpolarized light and light polarized with its E vector

perpendicular to the [100] direction of the sample are pretty well the same. Therefore, no dichroism has been observed on this sample within an estimate of the limit of error (factor 2). The conclusion to be reached that given a better sample, the technique may be a usable research tool for examining defects which would give reasonable dichroism ($>$ 10%).

Table I is a summary of the energy levels we have observed. As can be seen, the .26 eV and the .83 eV levels have been seen in samples of all types though not necessarily in all samples. We will not attempt to draw any conclusions about any of these levels now as we are still in the initial stages of the study and many are possible.

We next plan to irradiate some lower resisitvity material (1 Ωcm and possibly more 10 Ωcm) at both 1 and 50 MeV to study these. In this way, we hope to be able to introduce more defects without driving the resistance too high for ease in measurement.

3. Impurity Associated Defects in Silicon - R. Edelstein

Infrared and electrical studies of single crystal silicon bombarded with 48 MeV electrons were used to evaluate damage to various samples. Thirty (30) samples were prepared by conventional methods in either bar or bridge from. The bar samples used in the infrared experiments were 2 x 5 x 15 mm in dimensions having optical surfaces prepared using 0.3 micron alumina for the final polish. The bridge samples for electrical study were prepared using an ultrasonic cutter and the final etch was acid of the consistancy 1 HF_3: 3 HNO_3. Eighteen (18) samples were irradiated

TABLE I

PHOTOCONDUCTIVITY LEVELS OBSERVED:

100Ω cm P-doped	10Ω cm P-doped	100Ω cm Sb-doped	100Ω cm As-doped
		Ec-.22eV	
Ec-.26eV	Ec-.26eV	Ec-.26eV	Ec-.26eV
Ec-.29eV			
		Ec-.30eV	
			Ec-.33eV
Ec-.40eV			
		Ec-.42eV	
		Ec-.60eV	Ec-.60eV
Ec-.83eV	Ec-.83eV	Ec-.83eV	Ec-.83eV
Ev+.83eV	Ev+.83eV	Ev+.83eV	Ev+.83eV

while cooled by distilled water whose temperatures varied from 50^{o} to 62^{o}C. The fluxes varied from 0.97×10^{18} e/cm^2 for the electrical samples, 1.93×10^{18} electrons/cm^2 for six infrared and 4.89×10^{18} electrons/cm^2 for the other six samples. Below are tabulated data regarding irradiated samples.

Sample Dopant	Resistivity (At 300^{o}K Before Irradiation Ωcm)
Bismuth	0.01
Boron	0.01
Arsenic	0.01
Arsenic	0.1
Phosphorous	0.01
Phosphorous	0.1

All samples were supposed to be floating zone silicon and were irradiated in the [111] direction. The electrical measurements were made at about ten (10) temperatures between room temperatures and liquid nitrogen (80^{o}K).

In the boron - and phosphorous - doped samples of low (0.01 Ω-cm) resistivity little damage was observed at any of the 3 fluxes. All other samples did indicate the presence of the divacancy at 3.46 and 3.64 microns when cooled to 80^{o}K. The 0.1Ω-cm P-doped samples reflect large change in resistance but infrared studies do not show marked damage. The 0.1 and 0.01 Ω-cm As doped samples reflect essentially the same (lack of) damage independent of flux and none of these samples indicate the "5.5 micron" band previously reported by Cheng and Becker.[1] The reason for this is possible overheating during irradiation with

subsequent annealing. The sample which reflects the most damage is the 0.01 Ω-cm Bi doped sample and it is believed that most of these absorptions are due to oxygen associated defects. These include two vibrational bands at 12.0 and 11.56 microns and a band at 6.35 microns. The model 621 Perkin-Elmer spectrophotometer was purged to rid the system of water vapor absorption in the 5 to 8 micron region. The first annealing has been accomplished using boiling distilled water (monitored by a conventional mercury thermometer) for an anneal time of 15 minutes.

Subsequent anneals will be accomplished using the oven and thermocouples and in the interim time samples will be stored in a freezer at about -20°C. The annealing experiments will be completed during the next six month period.

4. Saturation of the Fermi Level in Germanium Irradiated to High Doses of 50 MeV Electrons ($\sim$5-10 x 10^{18} e/cm^2) - W. H. Bolke

A. Introduction and Experimental Methods

Preliminary results on the electrical properties of heavily irradiated p-type germanium were given in the last progress report covering the period from 15 March 1966 to 15 October 1966. In this report we shall give some of our final results on this phase of our work, a detailed write-up in the form of a paper to be submitted for publication is now in the process of being completed.

Eight-arm bridge type samples suitable for conductivity and Hall effect measurements were prepared by ultrasonic cutting of

40-mil thick slices. The samples were polished and finally etched in white etch (3 HNO_3 : 1 HF). Leads were attached to the samples by means of Cerroseal solder. The samples were irradiated with approximately 50 MeV electrons. The sample temperature during irradiation was maintained below 50°C by immersing the samples in a flow of water circulated through a fan-cooled radiator. We obtained the electrical properties (conductivity and carrier concentration) from 80-320°K using an evacuable stainless steel dewar, and standard dc voltage measuring techniques. A 5500 gauss electromagnet with a 2¼ inch gap was utilized in the Hall effect measurement.

B. Results

0.58 ohm-cm Ge (In) These samples were first subjected to a dose of 1.8×10^{18} e/cm^2 and then 1.0×10^{19} e/cm^2 total integrated flux. The Fermi energy vs. temperature curves are shown in Fig. 6. The pre-irradiation Fermi level lies very close to the final saturation or ultimate level. It can be seen from Fig. 6 that the Fermi level was moved below its final value (at 295°K) in the first irradiation and in the second irradiation the Fermi level achieved its saturation or ultimate value. The plots given in Fig. 6 were constructed from the carrier concentration vs. temperature data. In Fig. 7 we show the temperature dependence of conductivity before irradiation and after irradiation to two different total doses. Note that the pre-irradiation resistivity at 296°K ($\frac{1000}{T} = 3.38$) dropped to 0.37 ohm-cm from 0.58 ohm-cm after the first irradiation. In the second irradiation the resistivity was stabilized at the saturation value of 0.49 ohm-cm.

0.056 ohm-cm Ge (Ga) This set of samples was exposed to one dose only 8.2×10^{18} e/cm^2 and as expected the Fermi level shown in Fig. 8 was elevated by electron bombardment from $E_v + 0.14$ eV to $E_v + 0.15$ eV. The latter value is not expected to be the saturation or ultimate position of the Fermi energy since the carrier concentration versus 1000/T curves, Fig. 9, do not indicate saturation, and based upon previous systematics further irradiation would move the Fermi energy at a higher energy than 0.15 eV from the top of the valence band.

0.003 ohm-cm Ge (Ga) Three total integrated fluxes were obtained for study in this sample series; they are 1.8×10^{18}, 2.2×10^{18}, and 1.04×10^{19} electrons/cm^2. The conductivity vs. 1000/T plots for the various irradiation doses are presented in Fig. 10. The decrease in conductivity with increasing dose corresponds to an elevation of the Fermi level toward the ultimate value in comparison to the results for the 0.056 ohm-cm and 0.58 ohm-cm material.

0.001 ohm-cm Ge (Ga) These samples, of the lowest resistivity tested, were subjected to two irradiations resulting in total integrated fluxes of 1.8×10^{18} and 1.0×10^{19} electrons/cm^2. The conductivity vs. 1000/T curves in Fig. 11 again show the decrease in conductivity with increasing flux to be expected as the Fermi energy approaches its ultimate value.

Determining the Fermi energies within a reasonable degree of accuracy could not be accomplished. For highly doped samples (resistivities of 0.003 and 0.001 ohm-cm), the Hall effect is

quite small. A possible solution to this problem is to apply a large magnetic field and high sample currents. The large magnetic fields (up to 5.5 kilogauss) were easily obtained, but applying a high sample current results in heating of the sample with a resulting loss of temperature control. The change in Fermi energy for this 0.001 ohm-cm sample was inferred from the change in conductivity, and a comparison with the results of other samples of higher resistivity.

Carrier Addition and Removal Rates in p-type Ge The study of a wide range of resistivity p-type Ge has given the following carrier addition rates: 30Ωcm (Indium) + 0.026 carriers added/cm, a value of + 0.026 cm^{-1} (Indium)was measured for 10Ω -cm material. For low resistivity p-type material we measure carrier removal rates of -0.072 cm^{-1} for 0.003 Ω-cm (Gallium) and -0.1 cm^{-1} for 0.001Ω-cm Gallium-doped Germanium. The 0.57Ω-cm samples were too close to the saturation that the resistivity remained essentially constant during bombardment and we could not measure meaningful carrier removal or addition rates.

C. Disucssion of Results

The behavior of the conductivity of the 0.58 ohm-cm indium-doped germanium samples has been attributed to the proximity of the initial Fermi level to the ultimate level, leading to saturation of the hole concentration. Klontz[2] concluded that this saturation is due to the break-up of a complex defect formed by irradiation, which acts as an acceptor state at about E_v + 0.22 eV, and further irradiation has little effect on the saturated value of the hole concentration.

For low purity material, the initial Fermi level is quite low (below E_v + 0.1 eV), and the formation of the above defect may not be favorable due to a different charge state. This, along with measured carrier removal rates, may serve to explain why saturation is not observed for the low resistivity material.

As stated above, the determination of the Fermi energy for the low resistivity samples could not be performed. However, the increase in resistivity upon bombardment serves as an excellent indication of the upward trend of the Fermi energy, and, as such, is in agreement with the fast neutron bombardment results.(3)

Attainment of what is referred to as the ultimate Fermi level was not accomplished for the samples with resistivities of 0.056, 0.003, and 0.001 ohm-cm. Consequently, no value is presented for the total integrated flux necessary to achieve the ultimate Fermi level. If this level is associated with saturation of the carrier concentration, it may not be attainable from the standpoint of complex defect formation. However, if this level is to be found in low resistivity material, it must come only after prolonged bombardment by the fast neutrons. The experimentally determined carrier removal rate, 0.1 carriers removed/cm. for 0.001 ohm-cm gallium doped germanium, one would require on the order of 10^{20} electrons/cm^2 total integrated flux to achieve the ultimate level.

For the samples which attained saturation, it is possible to present values for the ultimate Fermi energy for irradiation temperatures of 323°K. From Kalma's data, (ref. 4) the ultimate level is 0.225 $\pm$ 0.010 eV above the valence band for 30 ohm-cm

indium-doped germanium. For 0.58 ohm-cm material of the same doping, the level is found to be 0.214 $\pm$ 0.010 eV above the valence band. This is to be compared with a value of E_v of 0.120 $\pm$ 0.006 eV in fast neutron irradiation of p-type germanium of several resistivities.[3]

The differences between the fast electron and fast neutron results most probably arises from the amount of disorder effected by the different particles. It has been shown that high energy electrons are capable of producing disordered regions or defect clusters in germanium.[5] More specifically, in n-type germanium, these fast electrons of about 50 MeV produce disordered regions of the same type observed with fast neutrons.[5]

It is reasonable to assume that fast electrons are capable of producing disordered regions in p-type germanium also, so that it remains to explain the difference with the ultimate value of the Fermi energy for fast neutron bombardment. Previous studies using 10 MeV deuterons incident upon p-type germanium at an irradiation temperature of -78^{o}C gave an ultimate value of E_v + 0.089 eV compared with E_v + 0.123 eV for fast neutrons.[6] A large part of this difference is ascribed to the much higher disordering rate of deuterons. Reverting once again to the fast electron-fast neutron results, one must then decide that the fast electrons produce less disorder in p-type germanium than

fast neutrons.

The association of defect electrical properties with the production of disordered regions which are unique to p-type germanium(50 MeV electrons) has not been demonstrated. This requires additional irradiations of a series of samples similar to those above by electrons with energies in the range 1-10 MeV where we would expect to show that disordered regions are not produced. It is expected, however , that the results will be similar in nature to those for n-type germanium subjected to 15 MeV electrons.[5]

The behavior of the conductivity of highly-doped p-type germanium has been clarified by this experiment. It was previously thought that the only effect produced by bombardment on the conductivity was through a decrease in mobility.[7] However, calculations based on measurements of the electrical properties of these samples show that the decrease in mobility is accompanied by a decrease in carrier concentration, both then combining to reduce the conductivity.

The calculation of carrier removal or additional rates can be seen to depend on the initial carrier concentration of the samples involved, the rate increasing for higher initial carrier concentrations. This agrees with the carrier removal rates obtained in p-type Ge under fast neutron bombardment,[6] with the expected result that the fast neutrons are more effective

than fast electrons in removing carriers.

D. Conclusions

The ultimate Fermi level was found to be $E_v + 0.214 \pm 0.010$ eV for 0.58 ohm-cm indium doped germanium. This is in good agreement with a value of $E_v + 0.225 \pm 0.010$ eV for 30 ohm-cm indium-doped germanium found in a previous study.

The ultimate Fermi level was not determined for samples of resistivity of 0.056 ohm-cm or less, since the hole concentration of these samples did not saturate upon irradiation. The increase in resistivity upon irradiation, corresponding to an increase in Fermi energy, is consistent with predicted behavior since the initial Fermi level of these samples lay below the ultimate value.

The position of the ultimate level for n-type germanium was determined to be $E_v + 0.23 \pm 0.01$ eV for 1 ohm-cm material and $E_v + 0.20 \pm 0.01$ eV for 0.1 ohm-cm material, independent of doping. These values compare well to those determined from p-type samples. Fast neutron[6] bombardment resulted in an ultimate Fermi level of 0.120 ± 0.003 eV for irradiation at 50°C while 10 MeV deuterons[6] produce an ultimate level of 0.089 eV at -78°C irradiation temperature. The difference in these results can be attributed to the difference in disordering properties of the bombarding particles. These results are shown in Fig. 12 and it appears that we can conclude that for irradiated germanium the ultimate

position of the Fermi level is characteristic of the nature of the disordered regions specifically, the greater the extent of the disordered region the closer the ultimate Fermi level lies to the valence band.

III. Research Plans for the Next Six Month Period

During the next 6-8 month period we shall plan to work on the following experiments:

1. The use of optical properties (including infrared absorption) to examine the systematics of impurity dependent radiation-induced defects.
2. Continued development of stress techniques coupled with dichroic measurements of photoconductivity in 1-50 MeV electron irradiated silicon.
3. Starting in June 1967 we shall spend a major portion of our effort studying the Li-defect complex in silicon.
4. Defects induced by 1 MeV boron and phosphorous ions in silicon.

References

1. L. J. Cheng, J. F. Becker, R.P.I. Progress Report to NASA covering period 15 September 1964 to 15 March 1965 for work on Grant NsG-290.

2. E. E. Klontz, J. W. MacKay, and T. W. Flanagan, Radiation Damage in Semiconductors (Dunod Cie, Paris 1965) p. 41.

3. J. W. Cleland, J. H. Crawford, Jr., K. Lark-Horovitz, J. C. Pigg, and F. W. Young, Jr., Phys. Rev. 84 861 (1951).

4. A. H. Kalma, private communication.

5. A. H. Kalma, J. C. Corelli, and J. W. Cleland, J. Applied Phys. 37 3913 (1966).

6. J. W. Cleland, J. H. Crawford, Jr., and J. C. Pigg, Phys. Rev. 99, 1170 (1955).

7. J. W. Cleland, J.H. Crawford, Jr., K. Lark-Horovitz, J. C. Pigg, and F. W. Young, Jr., Phys. Rev. 83, 312 (1951).

Figure Captions

Fig. 1 Photoconductivity spectra in the 1-4.5 μ range for a 100 Ω-cm arsenic-doped silicon sample irradiated at 300°K by 48 MeV electrons. The spectra shown were measured after 15 minute anneals at the indicated temperatures.

Fig. 2 Isochronal annealing (15 minutes at each temperature) of photoconductivity spectra for a 100 Ω-cm arsenic-doped silicon sample (F.Z.) irradiated by 48 MeV electrons at 300°K.

Fig. 3 Photoconductivity spectra in the 1 to 4.5 micron range after irradiation (48 MeV electrons at 300°K) and anneal for 15 minutes at the temperature shown for a 100 Ω-cm phosphorus-doped sample of floating zone silicon.

Fig. 4 Summary of isochronal annealing of photoconductivity spectra for a 100 Ω-cm phosphorus-doped silicon sample. The anneals are plotted for the photoconductivity of the various energy levels.

Fig. 5 Photoconductivity spectra for a 100 Ω-cm Sb-doped silicon sample measured after being stressed with 1400 kg/cm^2 along [011] at $\approx$150°C. The spectra were measured using light polarized along [100] and unpolarized light in order to search for dichroism (see the text) due to the divacancy defect.

Fig. 6 Temperature dependence of Fermi energy level in unirradiated and in $\approx$50 MeV electron-irradiated(at $\approx$325°K)0.58Ω-cm Ge (In).

Fig. 7 Conductivity vs. $\frac{1000}{T}$ in unirradiated and in $\approx$ 50 MeV electron-irradiated (at $\approx$325°K) 0.58 Ω-cm Ge (In).

Fig. 8 Temperature dependence of Fermi energy level in unirradiated and in $\approx$ 50 MeV electron-irradiated (at $\approx$ 325°K) 0.056 Ω -cm Ge (Ga).

Fig. 9 Carrier concentration vs. $\frac{1000}{T}$ in unirradiated and in $\approx$50 MeV electron-irradiated (at $\approx$325°K) 0.056Ω-cm Ge(Ga).

Fig.10 Conductivity vs. $\frac{1000}{T}$ in unirradiated and in $\approx$ 50 MeV electron-irradiated (at $\approx$325°K) 0.003 Ω -cm Ge(Ga).

Fig.11 Conductivity vs. $\frac{1000}{T}$ in unirradiated and in $\approx$50 MeV electron-irradiated (at $\approx$325°K) 0.001 Ω-cm Ge (Ga).

Fig.12 The position of the ultimate value of the Fermi level at saturation for germanium bombarded by various particles as shown on the figure.

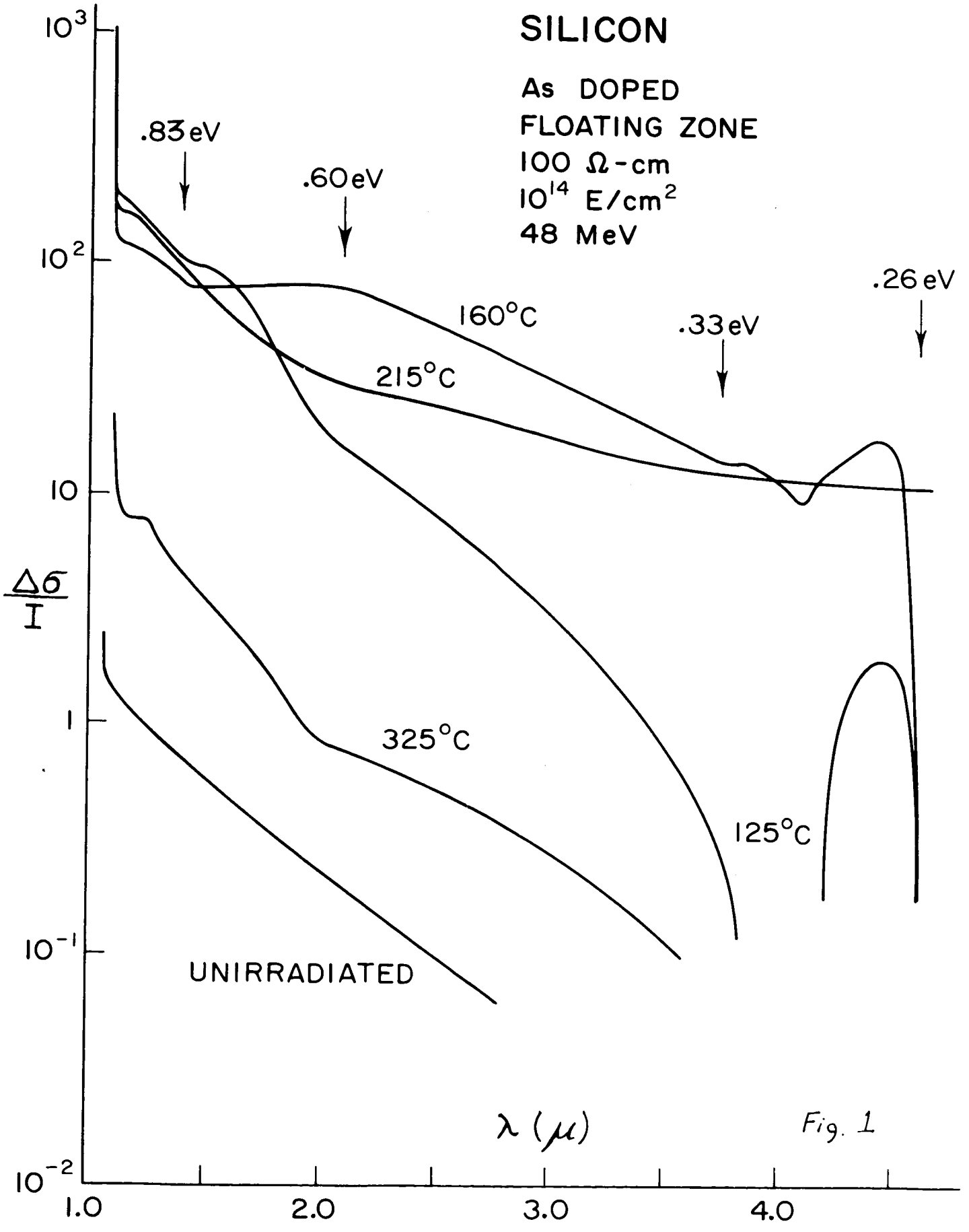
SILICON
As DOPED
FLOATING ZONE
100 Ω-cm
10^{14} E/cm^2
48 MeV
.83 eV
.60 eV
.33 eV
.26 eV
160°C
215°C
325°C
125°C
UNIRRADIATED
10^3
10^2
10
1
10^{-1}
10^{-2}
$\frac{\Delta\sigma}{I}$
1.0
2.0
3.0
4.0
λ (μ)

Fig. 1

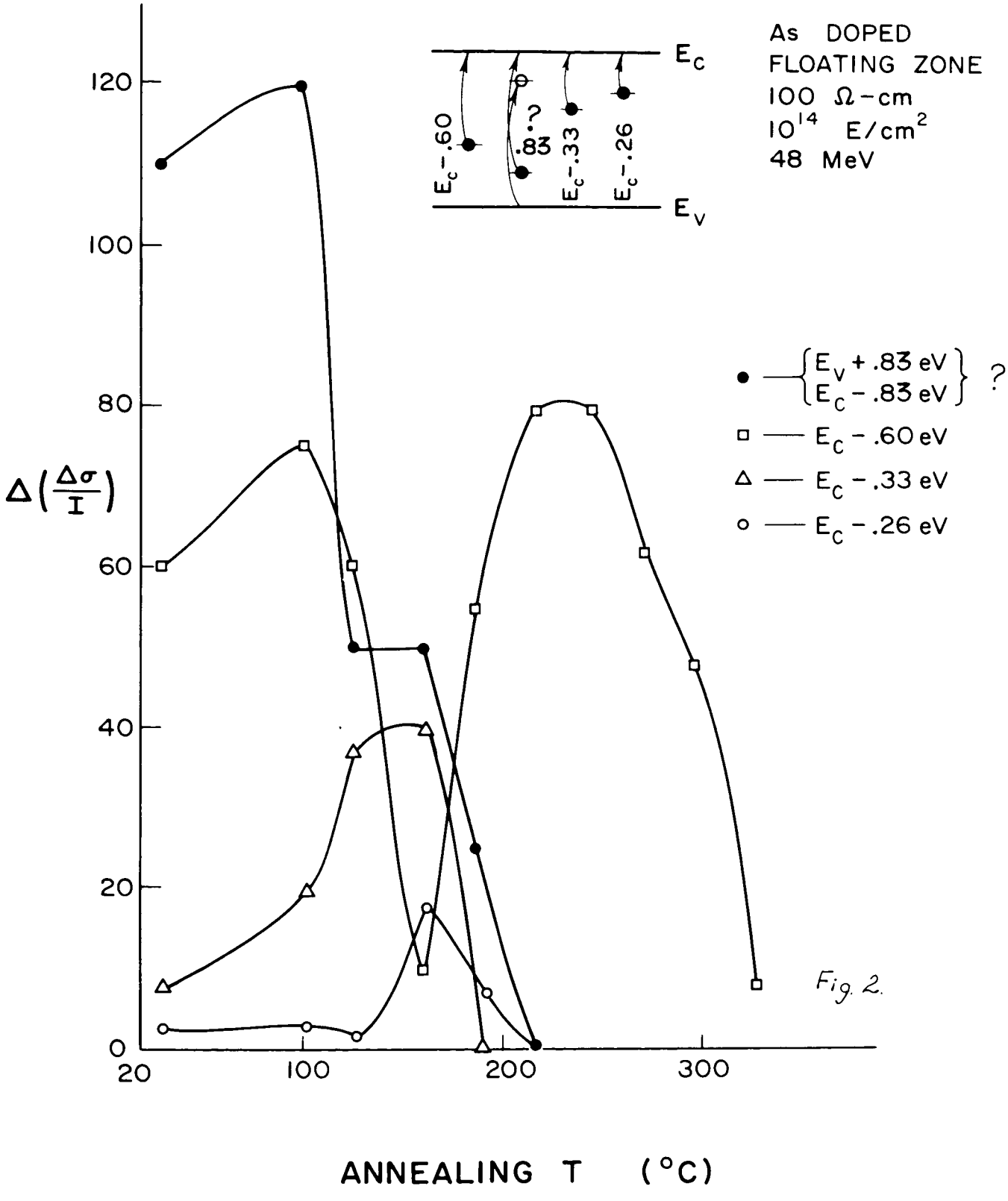
SILICON
As DOPED
FLOATING ZONE
100 Ω-cm
10^{14} E/cm^2
48 MeV
E_c
E_v
E_c-.60
.83 ?
E_c-.33
E_c-.26
$\Delta\left(\frac{\Delta\sigma}{I}\right)$
120
100
80
60
40
20
0
20
100
200
300
ANNEALING T (°C)
E_v + .83 eV
E_c - .83 eV
?
E_c - .60 eV
E_c - .33 eV
E_c - .26 eV

Fig. 2.

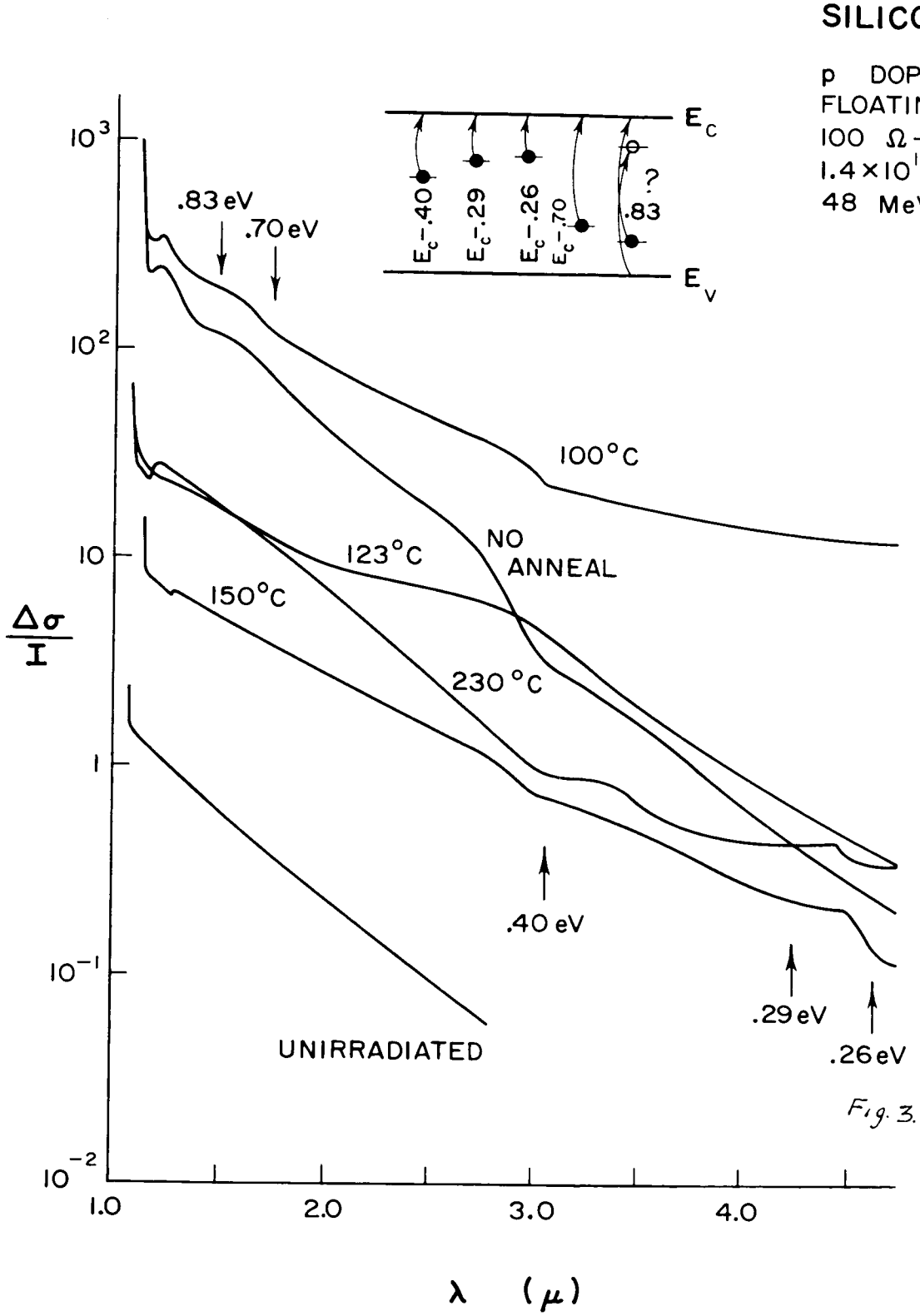
SILICON
p DOPED
FLOATING ZONE
100 Ω-cm
1.4×10^14 E/cm^2
48 MeV
E_C
E_V
E_c-.40
E_c-.29
E_c-.26
E_c-.70
?
.83
.83 eV
.70 eV
100°C
123°C
NO ANNEAL
150°C
230°C
.40 eV
.29 eV
.26 eV
UNIRRADIATED
Δσ/I
10^3
10^2
10
1
10^-1
10^-2
1.0
2.0
3.0
4.0
λ (μ)

Fig. 3.

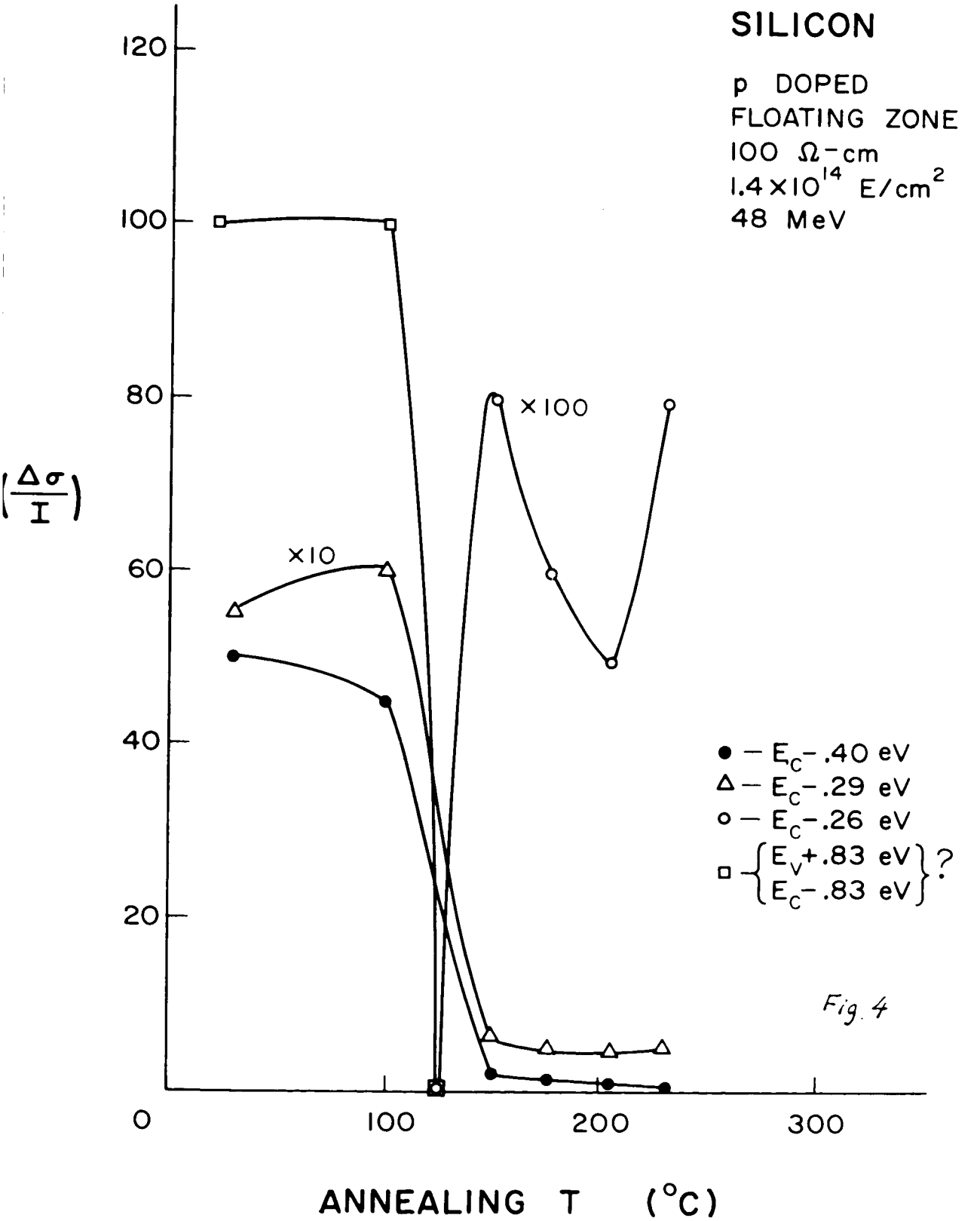
SILICON
p DOPED
FLOATING ZONE
100 Ω-cm
1.4×10^14 E/cm^2
48 MeV
120
100
80
60
40
20
0
100
200
300
(Δσ/I)
×100
×10
● — E_C - .40 eV
△ — E_C - .29 eV
○ — E_C - .26 eV
□ — {E_V + .83 eV / E_C - .83 eV} ?
ANNEALING T (°C)

Fig. 4

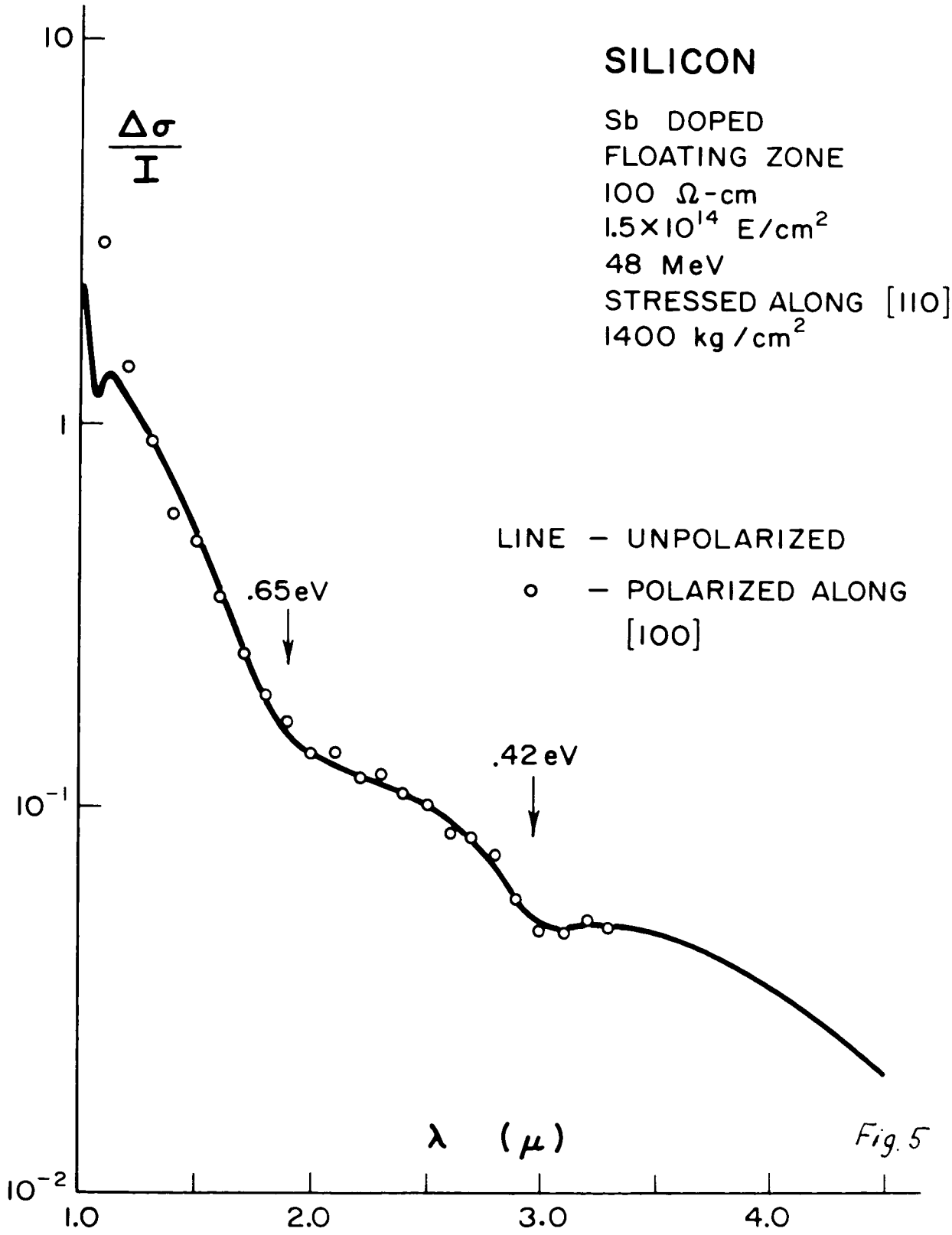
SILICON
Sb DOPED
FLOATING ZONE
100 Ω-cm
1.5×10^14 E/cm^2
48 MeV
STRESSED ALONG [110]
1400 kg/cm^2
LINE – UNPOLARIZED
o – POLARIZED ALONG [100]
Δσ/I
.65eV
.42eV
λ (μ)
10
1
10^-1
10^-2
1.0
2.0
3.0
4.0

Fig. 5

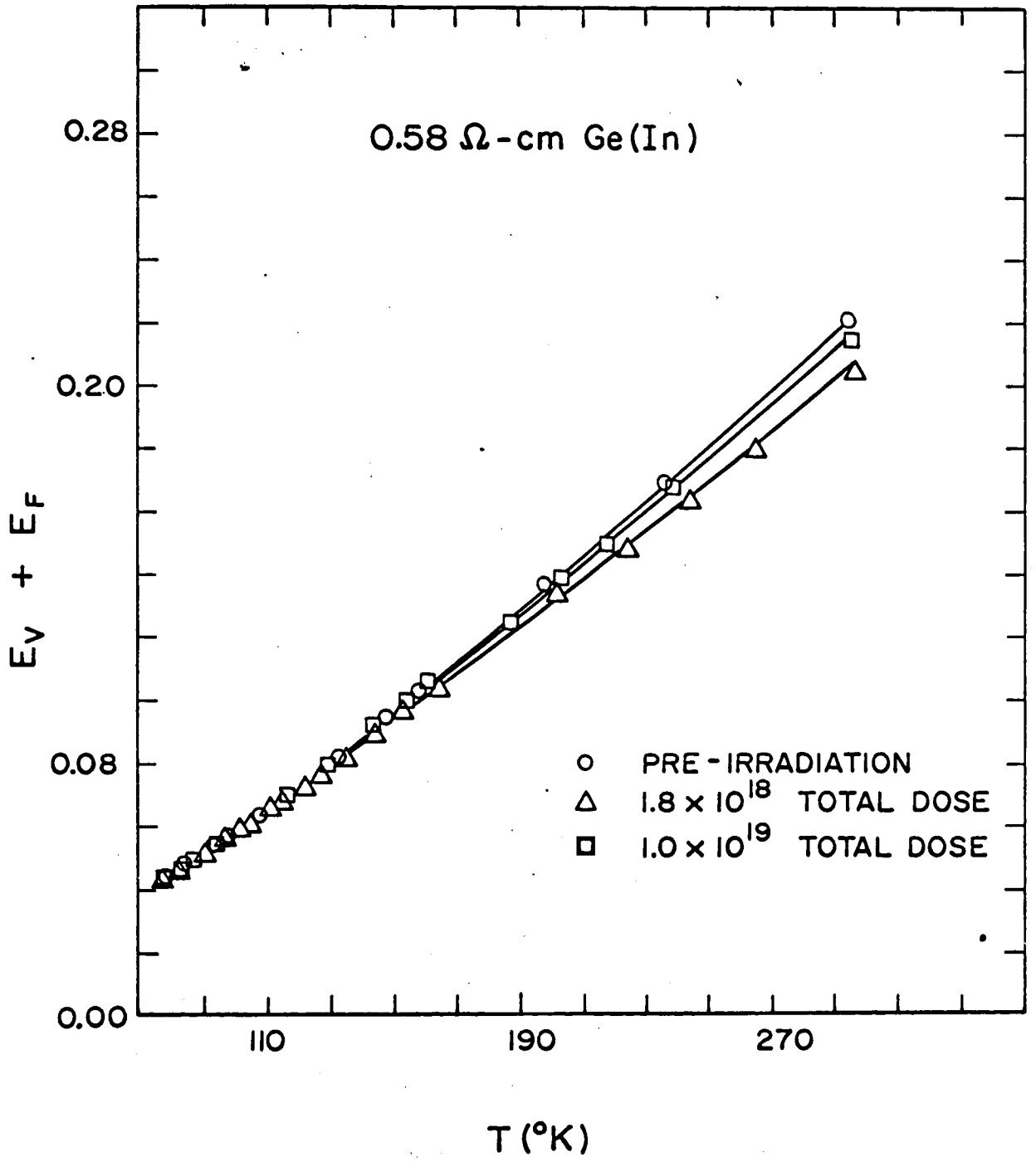
0.58 Ω-cm Ge(In)
0.28
0.20
0.08
0.00
$E_V + E_F$
110
190
270
T (°K)
PRE-IRRADIATION
1.8 × 10^18 TOTAL DOSE
1.0 × 10^19 TOTAL DOSE

Fig. 6

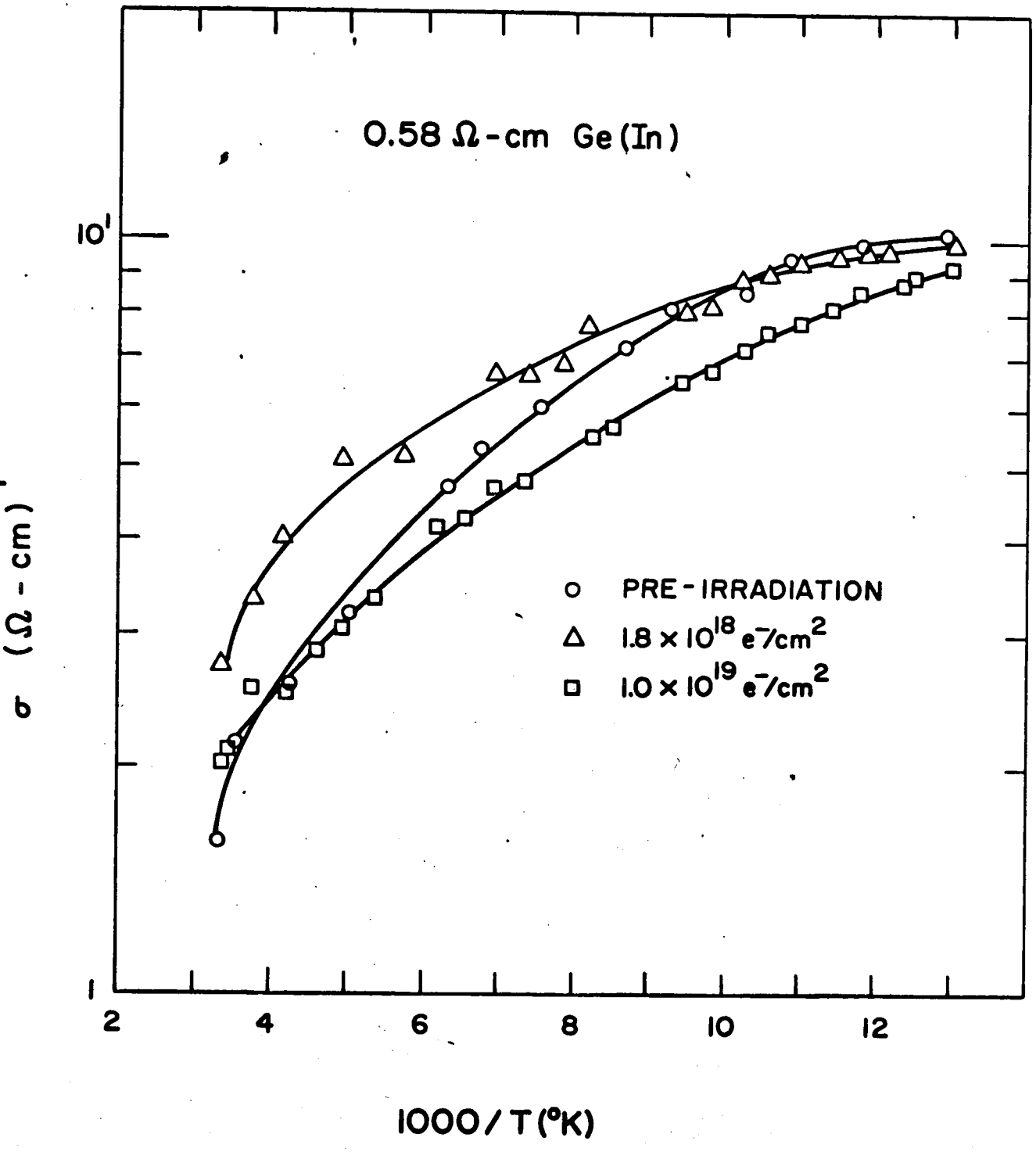
0.58 Ω-cm Ge(In)
10¹
1
2
4
6
8
10
12
σ (Ω-cm)⁻¹
1000/T(°K)
PRE-IRRADIATION
1.8 × 10¹⁸ e⁻/cm²
1.0 × 10¹⁹ e⁻/cm²

Fig. 7

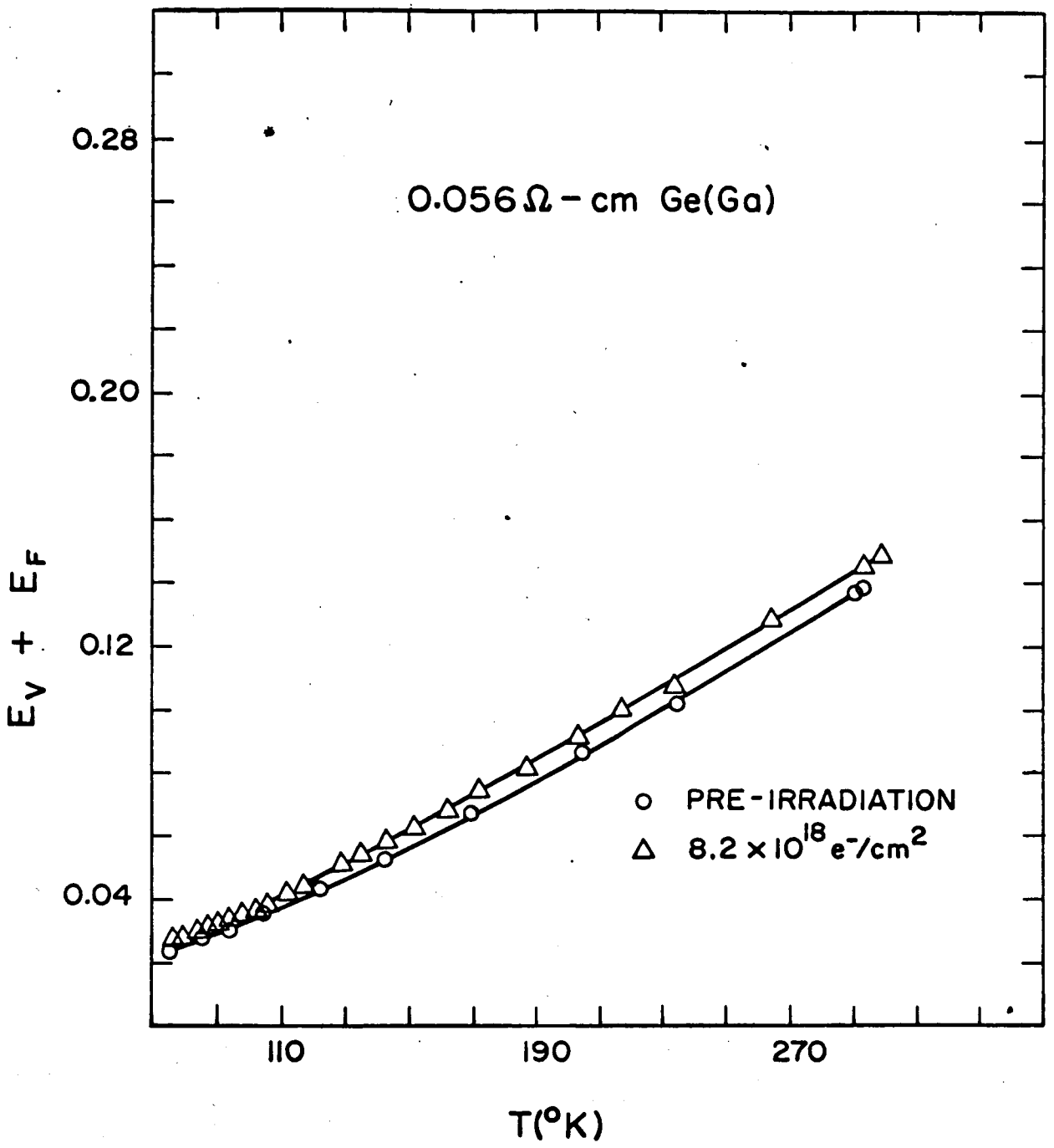
0.056 Ω – cm Ge(Ga)
0.28
0.20
0.12
0.04
$E_V + E_F$
110
190
270
T(°K)
PRE-IRRADIATION
8.2×10^{18} e⁻/cm²

Fig. 8

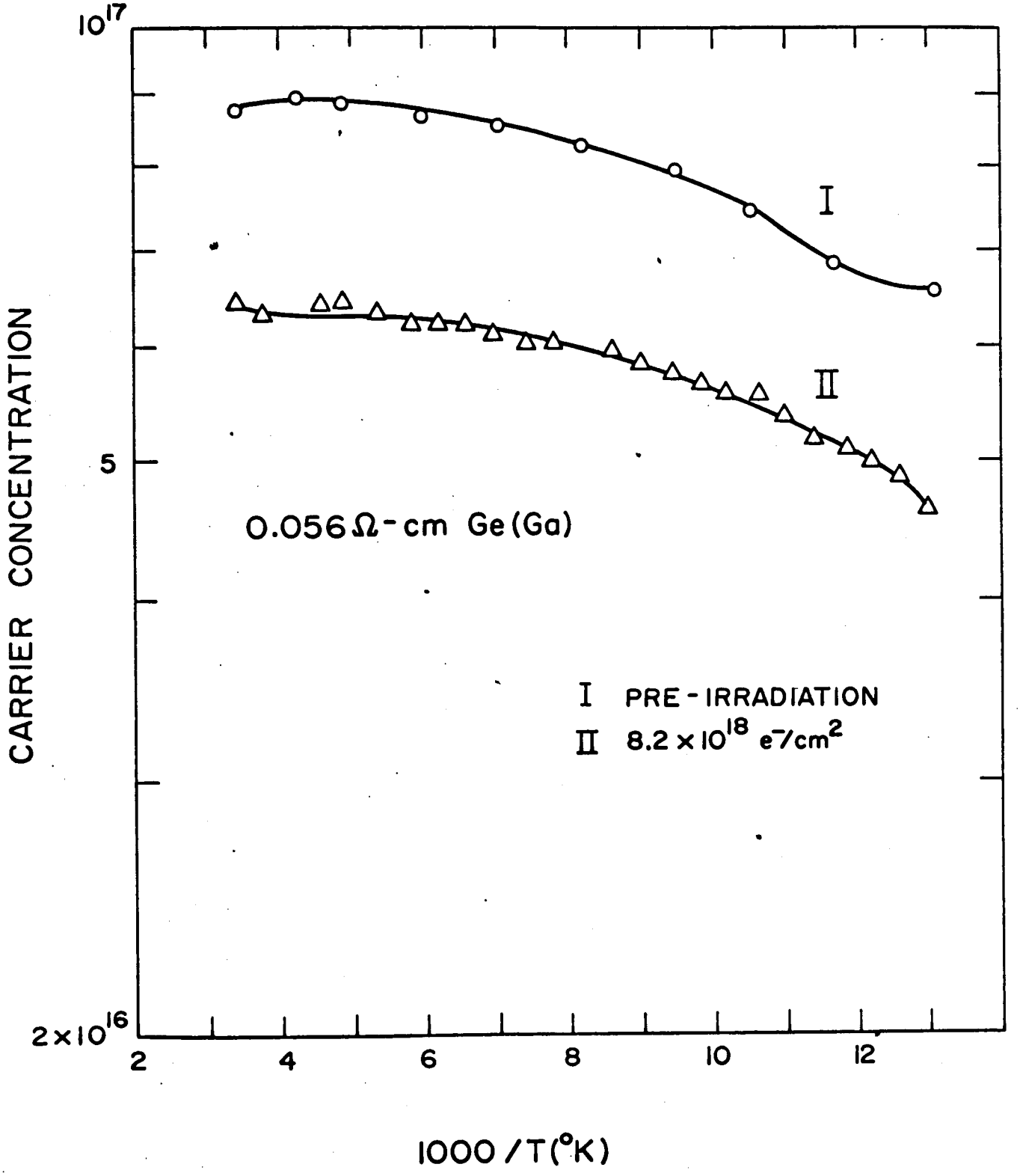
10^{17}
5
2×10^{16}
CARRIER CONCENTRATION
I
II
0.056 Ω-cm Ge(Ga)
I PRE-IRRADIATION
II 8.2×10^{18} e⁻/cm²
2
4
6
8
10
12
1000 / T(°K)

Fig. 9

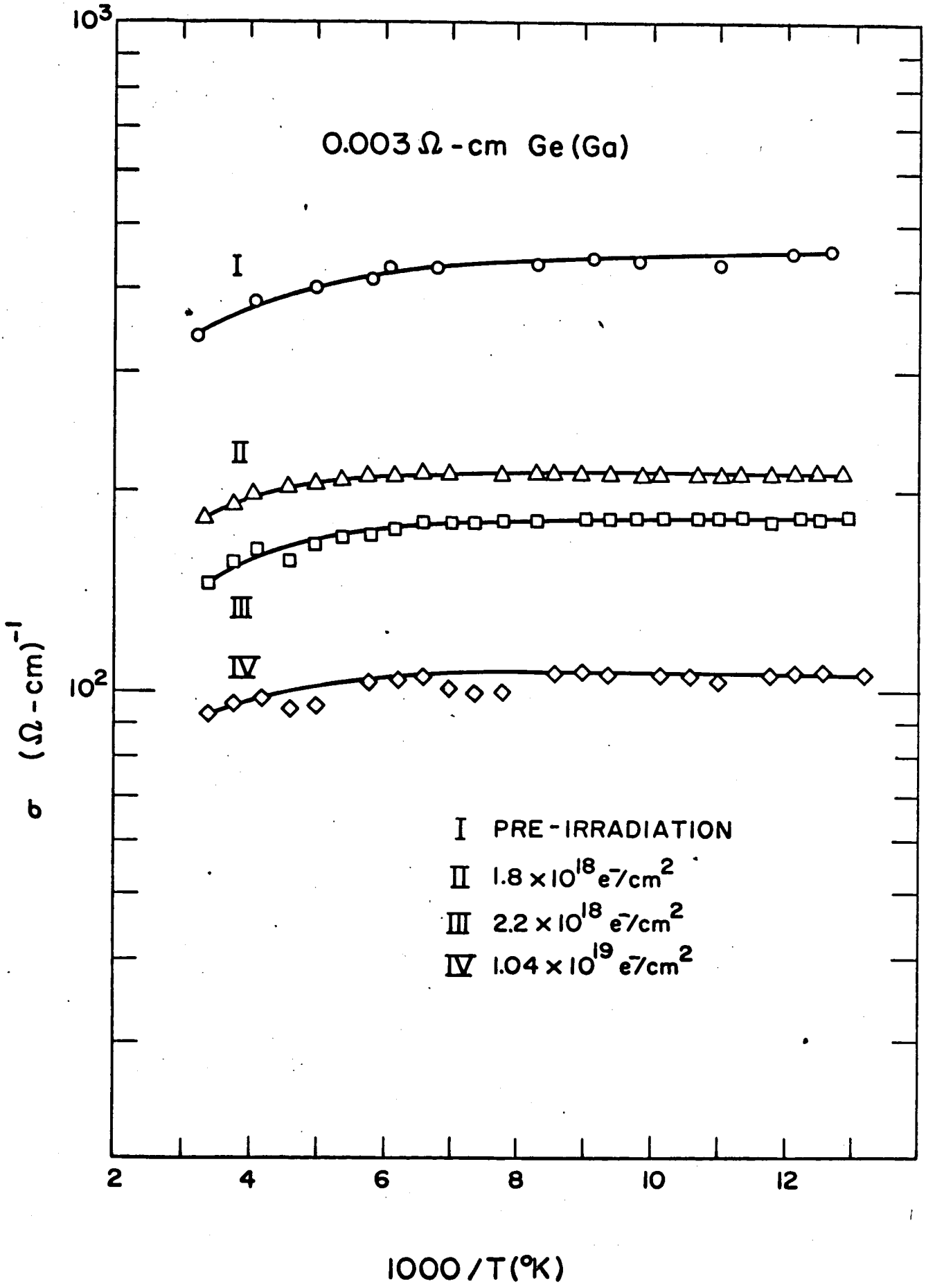
0.003 Ω - cm Ge (Ga)
I
II
III
IV
I PRE-IRRADIATION
II 1.8 x 10^18 e⁻/cm²
III 2.2 x 10^18 e⁻/cm²
IV 1.04 x 10^19 e⁻/cm²
σ (Ω-cm)⁻¹
10³
10²
2
4
6
8
10
12
1000/T(°K)

Fig. 10

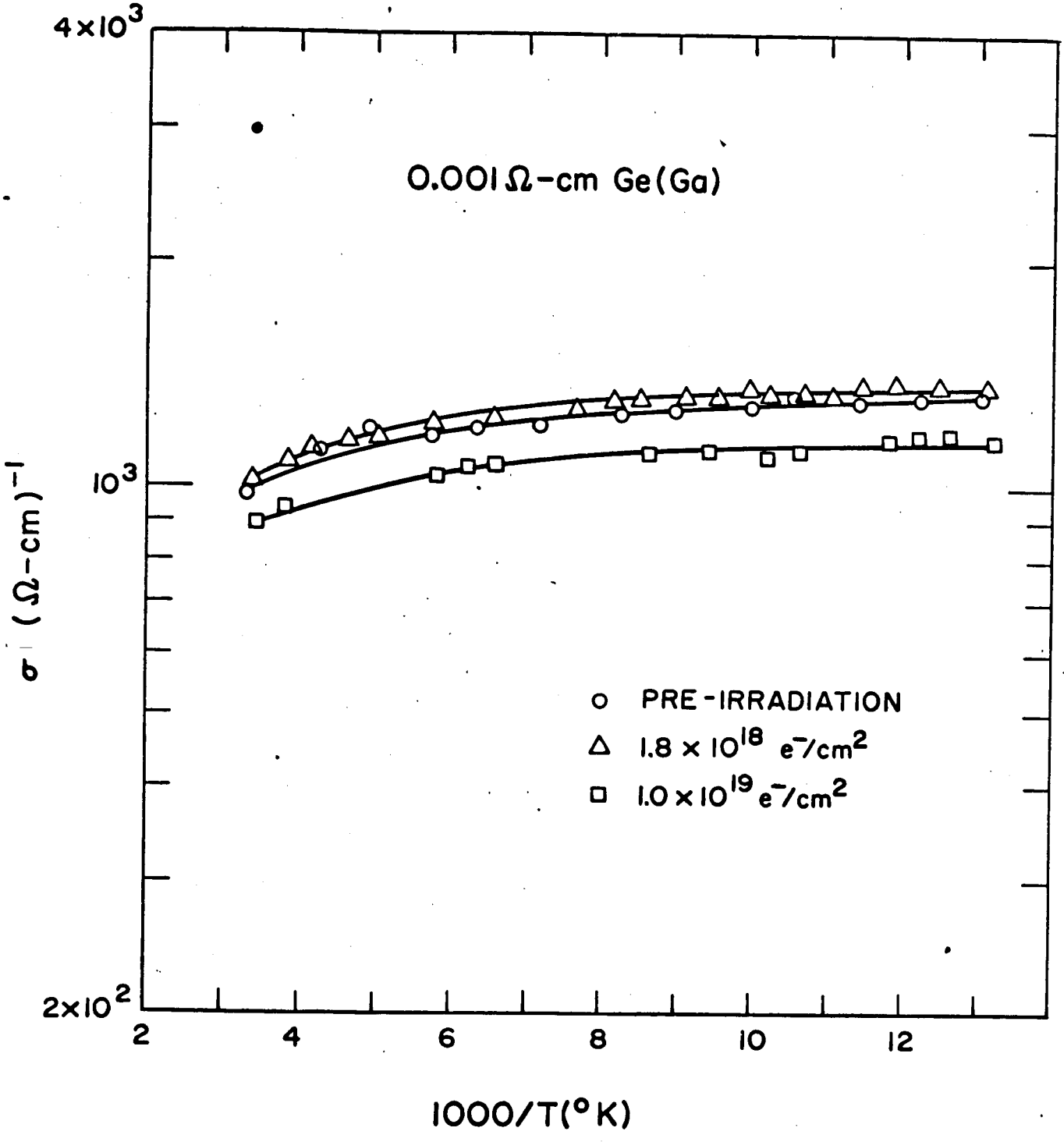
4×10^3
0.001 Ω-cm Ge(Ga)
10^3
σ (Ω-cm)^-1
PRE-IRRADIATION
1.8 × 10^18 e^-/cm^2
1.0 × 10^19 e^-/cm^2
2×10^2
2
4
6
8
10
12
1000/T(°K)

Fig. 11

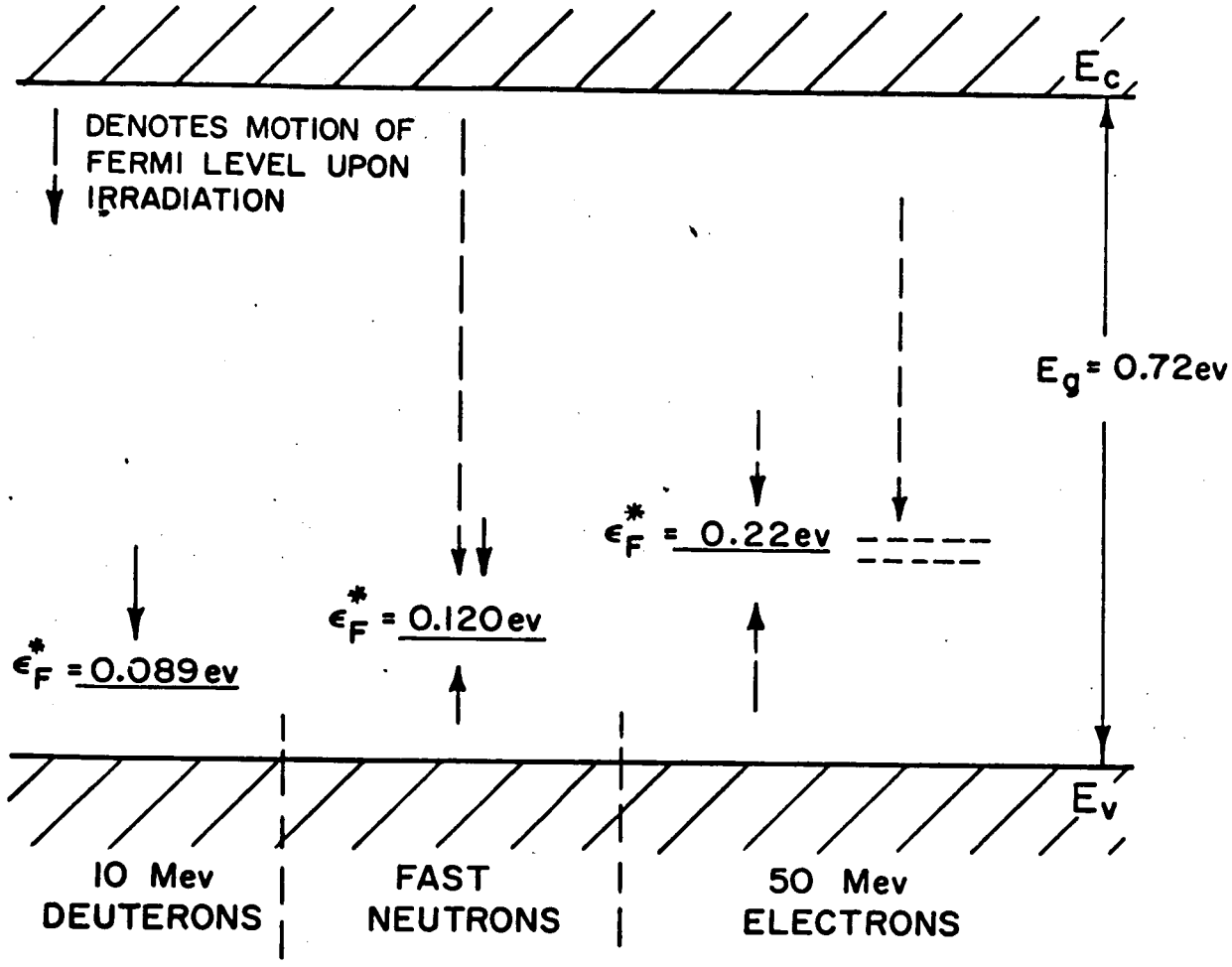

FINAL FERMI LEVEL AS A FUNCTION OF BOMBARDING PARTICLE

Fig. 12